JOURNAL OF MAGNETIC RESONANCE 40, 321–334 (1980)

Experimental Techniques of Two-Dimensional Correlated Spectroscopy

K. NAGAYAMA,*,† ANIL KUMAR,*,†,‡ K. WÜTHRICH,* AND R. R. ERNST†

*Institut für Molekularbiologie und Biophysik und †Laboratorium für Physikalische Chemie, Eidgenössische Technische Hochschule, 8093 Zürich, Switzerland

Received December 26, 1979

Two-dimensional (2D) homonuclear correlated spectra manifest connectivities between spin-coupled nuclei and can thus provide assignments of individual spin systems in complex ^{1}H NMR spectra. Two experimental techniques discussed in this paper, spin-echo correlated spectroscopy and foldover-corrected correlated spectroscopy, are particularly suitable versions for handling the large data matrices encountered in work with biological macromolecules. This paper explains the fundamental aspects of these two techniques and the relations with the conventional 2D correlated spectroscopy technique.

I. INTRODUCTION

Two-dimensional (2D) correlated spectroscopy, originally proposed by Jeener (*1*), is potentially an intriguing technique for the elucidation of connectivity among coupled nuclei (*2*). However, until quite recently, it has not been used extensively for the main reason that an enormous amount of data is required to compute a 2D correlated spectrum of a large- or even medium-sized molecule.

This situation has been changed recently by the recognition that in many situations the use of difference frequencies in one of the two frequency domains permits a significant reduction of the amount of data required (*3*). Several applications in our laboratories have shown that spin-echo correlated spectroscopy (SECSY) is a quite successful embodiment of this idea (*3*).

In this paper, we would like to demonstrate the connection between SECSY (*3*) and conventional 2D correlated spectroscopy (*1*, *2*), to discuss in some detail the experimental procedure and results, and to describe "foldover-corrected correlated spectroscopy" (FOCSY), another promising form of 2D correlated spectroscopy.

II. IMPLEMENTATION OF 2D CORRELATED SPECTROSCOPY

Conventional 2D correlated spectroscopy (*1*, *2*) employs a pair of 90° pulses (Fig. 1a). The first pulse, called the *preparation pulse*, serves to create transverse magnetization components for all allowed transitions. The following *evolution period* of length t_1 is required to "label" the various magnetization components

‡ On leave from the Department of Physics, Indian Institute of Science, Bangalore, India.

0022-2364/80/110321-14$02.00/0

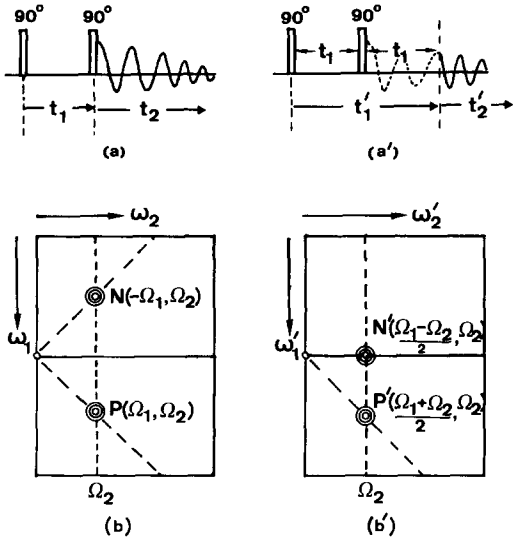

FIG. 1. The two schemes of 2D correlated spectroscopy. (a) conventional scheme (*2*); (a') spin-echo correlated spectroscopy scheme (*3*); (b) conventional 2D correlated spectrum showing two quadrants with *N*- and *P*-type peaks which are symmetry related; (b') corresponding 2D spin-echo correlated spectrum. Since $t_1' = 2t_1$, comparison of schemes a and a' might lead to the conclusion that SECSY has inherently lower sensitivity than conventional correlated spectroscopy. Since one is free in the choice of sampling points, this apparent limitation has no ill effects in practice.

with their characteristic precession frequencies. The second 90° pulse, the *mixing pulse*, causes transfer of magnetization components among all those transitions which belong to the same coupled spin systems. The ultimate distribution of labeled magnetization components is determined, finally, by measuring their new precession frequencies during the *detection period* (time variable t_2).

A 2D correlated spectrum can be considered as an autocorrelation diagram of a normal one-dimensional spectrum demonstrating the connectivity of transitions and of nuclei in coupled spin systems. The representation of such a 2D spectrum normally requires a quadratic matrix of dimension $F \times F$ where F is the chemical shift range covered by the spectrum. Such a matrix can require an excessively large set of data points, which may exceed the capacity of normally available computer systems, in particular for high-frequency spectroscopy with wide spectral ranges.

It has recently been recognized (*3*) that in many applications correlated resonance lines have rather close resonance frequencies so that most of the cross-peaks in a 2D correlated spectrum are located in a relatively narrow band along the main diagonal. By a suitable rearrangement (similarity mapping) of the 2D spectrum it is possible to considerably reduce the size of the matrix and to facilitate the practical application of 2D correlated spectroscopy using high-field spectrometers. In the following, we describe two practical implementations of such a rearrangement. SECSY achieves the rearrangement by a modified experimental scheme while FOCSY utilizes a special data processing technique.

(a) Spin-Echo Correlated Spectroscopy

The modified scheme required for SECSY (*3*) is indicated in Fig. 1a′. Here, the 90° mixing pulse is applied in the middle of the evolution period of length t_1', and the transfer of magnetization components occurs at $t = t_1'/2$. Let us consider the initially created magnetization of transition (mn). It will be transferred by the 90° pulse to, e.g., transition (kl). The average precession frequencies during the complete evolution period are then $\tilde{\omega} = \frac{1}{2}(\omega_{mn} \pm \omega_{kl})$. The sum frequencies can be suppressed by performing, in addition, a phase-shifted experiment. Details are explained in Section IV. The remaining difference frequencies $\tilde{\omega} = \frac{1}{2}(\omega_{mn} - \omega_{kl})$ often span a narrow frequency range in the ω_1 direction of the 2D spectrum. During the detection period the intrinsic precession frequencies lead to a full width F of the 2D spectrum in the ω_2 direction.

The potential of SECSY for delineating spin-coupling connectivities in protein ^{1}H NMR spectra is illustrated in Figs. 2 and 3. Figure 2 presents a three-dimensional visualization of the region from 0 to 6 ppm in the ^{1}H NMR spectrum of the basic pancreatic trypsin inhibitor (BPTI). Figure 3 presents a contour plot of the same spectrum and illustrates the analysis of a SECSY spectrum.

BPTI is a small globular protein with molecular weight 6500 which consists of one polypeptide chain of 58 amino acid residues. With the exception of the aromatic resonances of the four tyrosines and four phenylalanines, which we presented previously (*3*), the resonances of all nonlabile protons in BPTI are contained in the spectral region shown in Figs. 2 and 3. Connectivities between spin-coupled resonances are manifested in the following characteristic trait of a SECSY spectrum (*3*). Two spin-coupled resonances of nuclei A and X at $\Delta\delta = 0$, $\delta = \delta_A$ and $\Delta\delta = 0$, $\delta = \delta_X$, respectively, give rise to cross-peaks at the positions $\Delta\delta = \frac{1}{2}(\delta_A - \delta_X)$, $\delta = \delta_A$ and $\Delta\delta = \frac{1}{2}(\delta_X - \delta_A)$, $\delta = \delta_X$, where δ_A and δ_X are the chemical shifts of A and X. Hence the cross-peaks lie on a straight line which intersects the chemical shift axis at an angle of 135°. In Fig. 3 the connectivities are indicated for the resonances of four aliphatic amino acid residues which were previously identified by conventional one-dimensional NMR (*4, 5*). Threonine 32 gives rise to the highest-field methyl resonance at 0.59 ppm, which is connected with the β-proton line at 4.01 ppm, which is also coupled with the α-proton resonance at 5.28 ppm. The two methyl groups of valine 34 at 0.81 and 0.71 ppm are coupled with the β proton seen at 1.96 ppm, which in turn is connected also with the α-proton resonance at 3.92 ppm. The two A_3X spin systems of alanines 16 and 27 are seen to be identical within the resolution obtained in these experiments, with chemical shifts of 1.19 and 4.30 ppm for the methyl protons and the α proton, respectively.

A complete analysis of the spectra in Figs. 2 and 3, which provide connectivities between components of 30 spin systems, will be presented elsewhere (Nagayama, Ernst, and Wüthrich, to be submitted for publication).

(b) Foldover-Corrected Correlated Spectroscopy

FOCSY uses the basic experimental scheme of 2D correlated spectroscopy shown in Fig. 1a. The desired saving in experiment time and data storage is realized

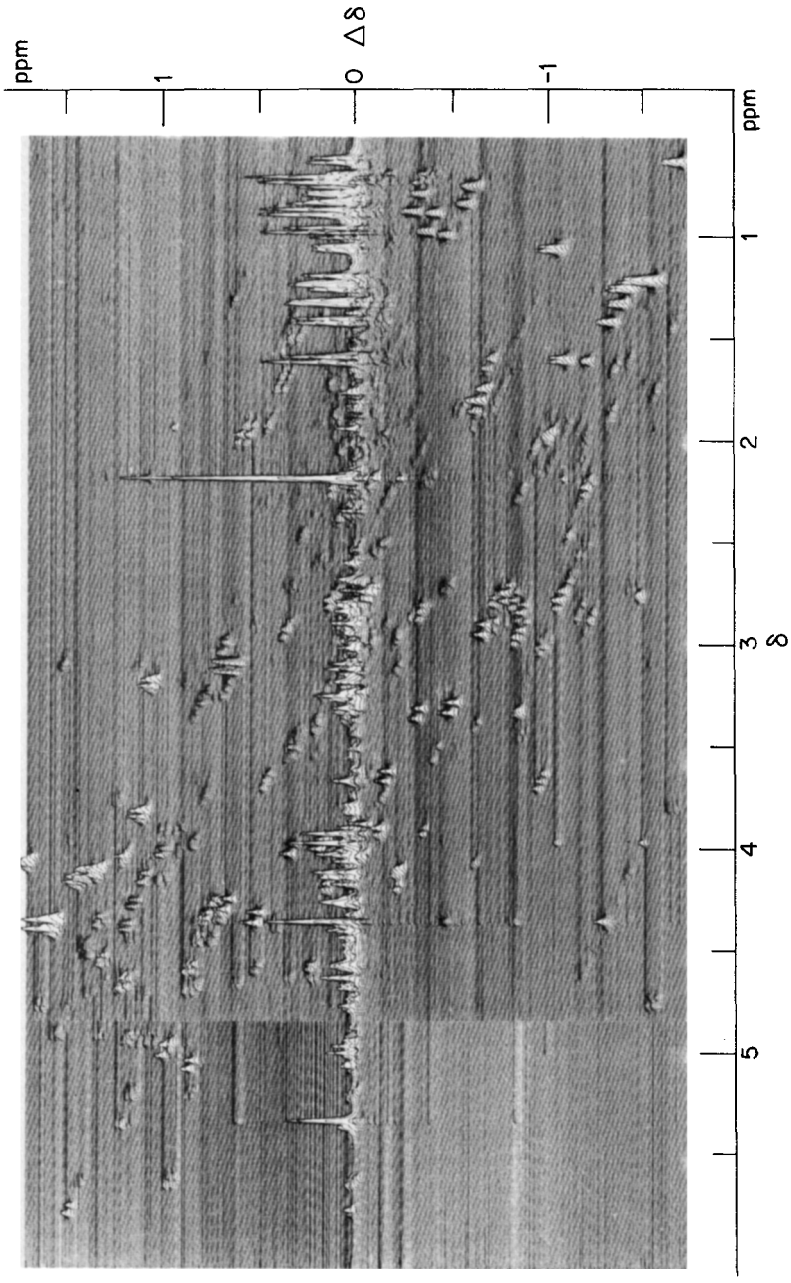

FIG. 2. Three-dimensional presentation of the spectral region from 0 to 6 ppm of a 360-MHz spin-echo correlated ^{1}H NMR spectrum recorded in a 0.01 *M* solution of the globular protein BPTI in "100%" D_2O, pH 7.0, T = 68°C. The chemical shift δ on the horizontal axis corresponds to that in conventional one-dimensional spectra. $\Delta\delta$ on the vertical axis stands for the difference frequencies between correlated nuclei. Cross-peaks between spin coupled nuclei are at $\pm\frac{1}{2}\Delta\delta$. The solvent singlet resonance is at 4.35 ppm. The apparent discontinuity at 4.8 ppm resulted since the spectrum, for practical reasons, had to be plotted in fragments extending over approximately 4 ppm.

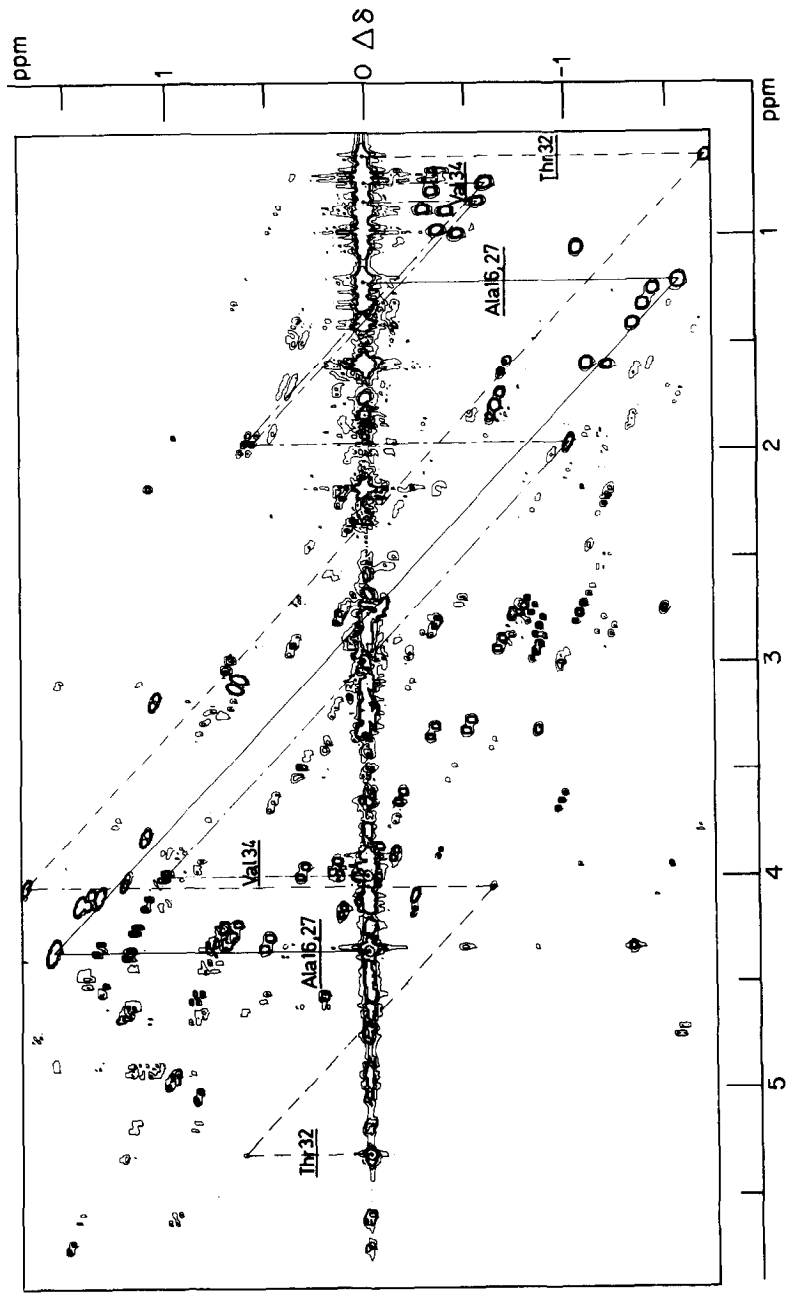

FIG. 3. Contour plot of the spin-echo correlated ^{1}H NMR spectrum of Fig. 2. Connectivities between the components of the following spin system are indicated: (----) Thr 32; (——) Val 34; (——) Ala 16 and Ala 27 (*4*, *5*).

by a coarse sampling on the t_1 time axis. In this, the sampling theorem (*6, 7*) is violated, which causes foldover of the 2D spectrum in the ω_1 direction. In most situations such foldover is fatal for the unequivocal interpretation of a spectrum. However, quite recently, Müller (*8*) has shown in the context of 2D resolved ^{13}C spectroscopy that under certain conditions a removal of foldover can be achieved by a quite simple data rearrangement procedure after 2D Fourier transformation. This idea can also be used in 2D correlated spectroscopy.

The basic principle of FOCSY is visualized in Fig. 4 which shows a hypothetical spectrum corresponding to three pairs of coupled spins with differences of Zeeman frequencies $|\omega_i - \omega_k| = 3$, 4, and 2, respectively. Figure 4a shows the original 2D correlated spectrum in which foldover occurred in the ω_1 direction at the Nyquist frequency $\omega_N = 1/2$ because of coarse sampling along t_1. The foldover can be seen from the fact that the main diagonal is broken. The corresponding FOCSY spectrum is given in Fig. 4b. Here, the main diagonal has been reconstituted and put along the new ω_2' axis. The cross-peaks appear at positions reminiscent of those in a SECSY spectrum. However, the scale in the ω_1' direction is twice that of a SECSY spectrum. As a consequence, related cross-peaks appear therefore at an angle of 116.6° instead of 135°.

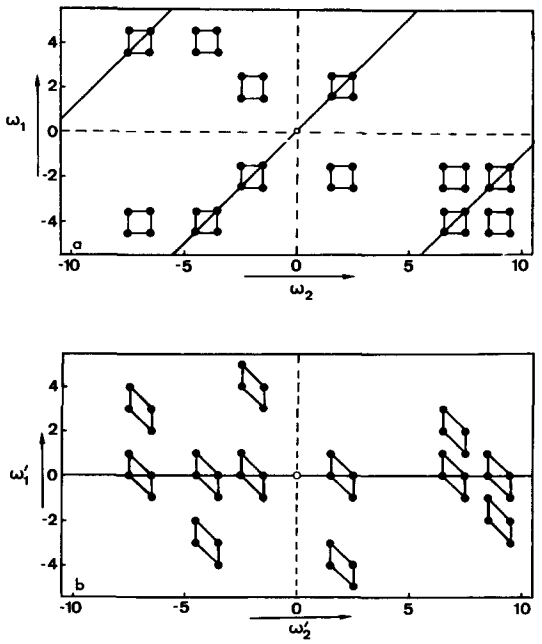

FIG. 4. The principle of FOCSY. (a) 2D correlated spectrum with foldover in the ω_1 direction. Foldover is visible by the solid line which indicates the broken main diagonal. (b) Foldover-corrected spectrum obtained from (a) by a cyclic rotation of the data points within each data column by its value of $-\omega_2$. Note that the direction of ω_1 is opposite to that in Figs. 1 to 3 and 5. This choice is necessary to obtain a FOCSY spectrum directly comparable to a SECSY plot.

To obtain Fig. 4b from Fig. 4a, the data within each data column must be rotated by a number of places given by the corresponding value of $-\omega_2$. The sense of rotation is determined by the sign of $-\omega_2$. This is a very simple mathematical procedure. Let us consider as examples the operation for some of the multiplet centers of Fig. 4.

(ω_1,ω_2)	$(\omega_1 - \omega_2, \omega_2)$	(ω_1', ω_2')
(−2,−2)	(0,−2)	(0,−2)
(2,−2)	(4,−2)	(4,−2)
(4,−7)	(11,−7)	(0,−7)
(−4,−7)	(3,−7)	(3,−7)
(−2,7)	(−9,7)	(2,7)

The rearrangement procedure of the originally computed spectrum $S(\omega_1,\omega_2)$ into a foldover-corrected spectrum $S'(\omega_1',\omega_2')$ can also be formulated in mathematical terms as follows:

$$S'(\omega_1',\omega_2') = S(\omega_1,\omega_2) \qquad [1]$$

with:

$$\omega_1' = (\omega_1 - \omega_2 + \omega_N) \bmod 2\omega_N - \omega_N,$$

$$\omega_2' = \omega_2.$$

This rearrangement ensures that ω_1' lies within the Nyquist frequency, $-\omega_N < \omega_1' < \omega_N$.

It is important to recognize that foldover correction is possible only when positive and negative ω_1 frequencies can be distinguished. This requires the performance of two independent recordings for each t_1 value with the second 90° pulse phase-shifted by 90°, i.e.,

Experiment 1: $\left(\frac{\pi}{2}\right)_x$, t_1, $\left(\frac{\pi}{2}\right)_y$, acquisition,

Experiment 2: $\left(\frac{\pi}{2}\right)_x$, t_1, $\left(\frac{\pi}{2}\right)_x$, acquisition.

In addition, it is of advantage to distinguish also positive and negative frequencies in ω_2 by means of quadrature phase detection.

(c) Comparison of the Two Techniques

Both methods have characteristic properties which we would like to point out.

(i) Attainment of pure phase. SECSY has a strong relation to 2D *J*-resolved spectroscopy (*9–11*). It is known that in homonuclear 2D *J*-resolved spectroscopy it is not possible to separate 2D absorptive and 2D dispersive lineshapes (*12*). The same is true also for SECSY. The basic reason for this fact is the absence of a phase-selection pulse at the end of the evolution period. FOCSY, however,

uses the unmodified basic pulse sequence of 2D correlated spectroscopy and permits clean phase separation.

Phase separation is of advantage when ultimate resolution must be achieved as the dispersive contribution necessarily leads to line broadening. This feature, however, should not be overemphasized as 2D correlated spectra of complex molecules are normally restricted to relatively low resolution because of limitations of the available data set and of measuring time.

(ii) Experimental technique. Two-dimensional correlated spectroscopy will often be used side by side with 2D *J*-resolved spectroscopy (Nagayama, Ernst, and Wüthrich, to be submitted for publication). In this context SECSY has the inherent advantage that a minimum number of changes to a 2D *J*-resolved spectroscopy program must be made for its realization.

(iii) Storage and computational requirements. The requirements with respect to data storage and to computation time are very similar in the two techniques.

Although no FOCSY experiments have yet been performed, it can be expected that in practical applications performance of both techniques is very similar and that the inherent differences do not become apparent in typical spectra.

III. RELATION BETWEEN SPIN-ECHO CORRELATED SPECTROSCOPY AND CONVENTIONAL 2D CORRELATED SPECTROSCOPY

We would like to illuminate further the relation between the two types of presentation of a 2D correlated spectrum from the mathematical side. The clue to understand the relationship between conventional 2D correlated spectroscopy and SECSY, illustrated schematically in Figs. 1a and a′, is the similarity theorem (*6, 7*) which asserts that Fourier transform pairs conserve their functional forms under a similarity transformation.

If

$$f(t) \overset{\mathcal{F}}{\longleftrightarrow} F(\omega), \qquad [2]$$

then

$$f(at) \overset{\mathcal{F}}{\longleftrightarrow} \frac{1}{|a|} F(\omega/a). \qquad [3]$$

The similarity theorem can easily be extended to n-dimensional Fourier transforms:

If

$$f(\mathbf{t}) \overset{\mathcal{F}^n}{\longleftrightarrow} F(\tilde{\boldsymbol{\omega}}) \qquad [4]$$

then

$$f(A\mathbf{t}) \overset{\mathcal{F}^n}{\longleftrightarrow} \frac{1}{|A|} F(\tilde{\boldsymbol{\omega}} A^{-1}). \qquad [5]$$

Here, A is the matrix of the similarity transformation, $\mathbf{t}$ is the n-dimensional column vector of time variables, and $\tilde{\boldsymbol{\omega}}$ is the n-dimensional row vector of frequency variables; $|A|$ represents the determinant of A.

The two schemes shown in Figs. 1a and a′ differ in the definition of the time variables t_1, t_2 and t_1', t_2'. The following connection is found between the two

impulse response functions $s(t_1,t_2)$ and $s'(t_1',t_2')$ of correlated spectroscopy and of SECSY, respectively:

$$s(t_1,t_2) = s'(t_1',t_2') = s'(A\mathbf{t}),$$
$$A = \begin{bmatrix} 2 & 0 \\ -1 & 1 \end{bmatrix}, \quad A^{-1} = \begin{bmatrix} ½ & 0 \\ ½ & 1 \end{bmatrix}, \qquad [6]$$
$$\mathbf{t} = \begin{pmatrix} t_1 \\ t_2 \end{pmatrix}.$$

Applying the n-dimensional similarity theorem to the above equation, we can derive a relationship which connects the two corresponding spectra,

$$S(\omega_1,\omega_2) = \frac{1}{|A|} S'(\tilde{\omega}A^{-1})$$
$$= \frac{1}{2} S'\left(\frac{\omega_1 + \omega_2}{2}, \omega_2\right), \qquad [7]$$
$$\tilde{\omega} = (\omega_1,\omega_2).$$

Equation [7] expresses the fact that a SECSY spectrum can be obtained by a similarity mapping from a conventional 2D correlated spectrum. These considerations are correct as far as the signal frequencies are concerned. However, considerations of the resulting lineshapes are more subtle. This arises from the fact that the two data sets in the time domain are not identical since in SECSY, signal observation starts only following a time lag t_1 after the mixing pulse (Fig. 1). We do not discuss here the consequences for the lineshapes.

The similarity theorem allows us also to understand the appearance of a set of unexpected peaks in a SECSY spectrum. They occur unless a special phase alternation scheme is used, which will be described in the next section. Let us assume a single-phase experiment which does not permit the distinction of positive and negative ω_1 frequencies in a 2D correlated experiment. It produces a duplication of the peaks in the positive and negative ω_1 frequency domain. This is indicated in Fig. 1b by the two peaks $P(\Omega_1,\Omega_2)$ and $N(-\Omega_1,\Omega_2)$. A similarity mapping according to Eq. [7] again produces two peaks in the SECSY spectrum shown in Fig. 1b′. The peak designated as $N'((\Omega_2 - \Omega_1)/2, \Omega_2)$ belongs to the desired set while $P'((\Omega_2 + \Omega_1)/2, \Omega_2)$ appears at a high ω_1' frequency and will in most cases lead to foldover. Aliasing problems can be prevented by a suppression of the P' peaks.

In more physical terms, one may say that the $\pi/2$ mixing pulse leads to terms with apparent positive and negative time evolution during the first half of the evolution period. The term with apparent negative time evolution causes the desired peaks at the difference frequencies while the term with the apparent positive time evolution leads to additive precession angles during the two halves of the evolution period and must be suppressed to obtain a clean SECSY spectrum.

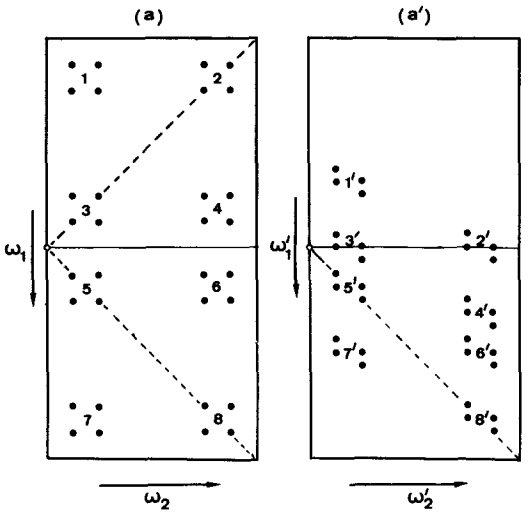

FIG. 5. The relation between the conventional 2D correlated spectrum and the SECSY of an AX two-spin system. (a) 2D correlated spectrum obtained by the scheme of Fig. 1a; (a') SECSY obtained by the scheme of Fig. 1a'.

IV. SUPPRESSION OF SUM FREQUENCY PEAKS IN SPIN-ECHO CORRELATED SPECTROSCOPY

Let us investigate the features shown in Figs. 1b and 1b' in more detail by considering the 2D spectra for the weakly coupled two-spin system represented in Fig. 5. The 2D correlated spectrum, given in Fig. 5a, consists of eight groups of four peaks. Half of the groups, numbered 1 to 4, belong to N-type peaks while peaks 5 to 8 are P-type peaks (compare Section III). There is an exact symmetry of N- and P-type peaks. The similarity mapping, according to Eq. [7], leads to the SECSY spectrum of Fig. 5a'. It is obvious that groups 1 to 4 contain the desired connectivity information while peaks 5 to 8 lead only to additional complications and possibly to foldover. They will be eliminated by the procedure to be described in the following.

Let us consider the effects of a phase change of the mixing pulse by $\pi/2$ by using the basic formalism of 2D correlated spectroscopy (*2*). The complex amplitude factor of a cross-peak between transitions (mn) and (kl) is given by

$$Z^{(x)}_{kl,mn} = F_{ykl} R^{(x)}_{lm} R^{(x)*}_{kn} F_{ymn}. \qquad [8]$$

Here, F_y is the y component of the total spin operator and $R^{(x)}$, explicitly given by $R^{(x)} = \exp(-i(\pi/2)F_x)$, is the rotation operator representing the mixing pulse. Now let us rotate the phase of the mixing pulse by $\pi/2$, replacing F_x by F_y in the rotation operator. This phase change can be expressed by

$$R^{(y)} = \exp\left(-i\frac{\pi}{2}F_z\right) R^{(x)} \exp\left(i\frac{\pi}{2}F_z\right). \qquad [9]$$

For $Z^{(y)}_{kl,mn}$ we obtain the following explicit expression using the magnetic quantum numbers of the involved states:

$$Z^{(y)}_{kl,mn} = \exp\{i[M_k - M_l]\pi/2 + i[M_m - M_n]\pi/2\} \times F_{ykl}R^{(x)}_{lm}R^{(x)*}_{kn}F_{ymn} \qquad [10]$$

$$= \exp\{i(\Delta M_{kl} + \Delta M_{mn})\pi/2\}Z^{(x)}_{kl,mn},$$

$$\Delta M_{kl} = M_k - M_l = \pm 1, \qquad \Delta M_{mn} = M_m - M_n = \pm 1.$$

One finds that for N-type peaks $\Delta M_{mn} = \Delta M_{kl}$ and therefore

$$Z^{(y)}_{kl,mn} = -Z^{(x)}_{kl,mn}. \qquad [11]$$

That is, a phase change of the mixing pulse by $\pi/2$ leads to a sign change of N-type peak amplitudes. On the other hand, for P-type peaks, $\Delta M_{mn} = -\Delta M_{kl}$, and

$$Z^{(y)}_{kl,mn} = Z^{(x)}_{kl,mn}. \qquad [12]$$

By subtraction of the response to a $(\pi/2)_y$ mixing pulse from that to a $(\pi/2)_x$ mixing pulse it is possible to eliminate the undesired P-type peaks.

It turns out that for practical applications it is worthwhile to use for each t_1 value a sequence of four recordings instead of the two recordings suggested by the above considerations:

$$\left(\frac{\pi}{2}\right)_x, \frac{t_1}{2}, \left(\frac{\pi}{2}\right)_x, \frac{t_1}{2}, \quad \text{acquisition } (+);$$

$$\left(\frac{\pi}{2}\right)_x, \frac{t_1}{2}, \left(\frac{\pi}{2}\right)_y, \frac{t_1}{2}, \quad \text{acquisition } (-);$$

$$\left(\frac{\pi}{2}\right)_x, \frac{t_1}{2}, \left(\frac{\pi}{2}\right)_{-y}, \frac{t_1}{2}, \quad \text{acquisition } (-);$$

$$\left(\frac{\pi}{2}\right)_x, \frac{t_1}{2}, \left(\frac{\pi}{2}\right)_{-x}, \frac{t_1}{2}, \quad \text{acquisition } (+).$$

With this scheme, it is possible also to eliminate, in addition to P-type peaks, the axial peaks (*2*) which originate from the mixing pulse and do not contain any connectivity information.

V. CALCULATION OF SPIN-ECHO CORRELATED SPECTRA

The similarity relation between SECSY and conventional 2D correlated spectra pointed out in Section III enables us to use the expressions derived for 2D correlated spectroscopy to compute SECSY spectra. The signal intensities are given by Eq. [8] and the line positions can be obtained by the similarity rules given in Section III. The lineshapes, however, differ from those of 2D correlated spectroscopy (*2*) where pure 2D absorptive or 2D dispersive lines are obtained. For SECSY, all lines are superpositions of equally weighted 2D absorptive and 2D dispersive contributions. Some of the peaks show positive, some negative peak intensities.

TABLE 1

PEAK INTENSITIES IN A SECSY SPECTRUM OF A STRONGLY COUPLED TWO-SPIN AB SYSTEM USING A 90°_x, $t_1'/2$, β°_x, $t_1'/2$, t_2' PULSE SEQUENCE

	ω_2			
ω_1	$\frac{1}{2}(\omega_A + \omega_B) - \frac{1}{2}D - \frac{1}{2}J$	$\frac{1}{2}(\omega_A + \omega_B) - \frac{1}{2}D + \frac{1}{2}J$	$\frac{1}{2}(\omega_A + \omega_B) + \frac{1}{2}D - \frac{1}{2}J$	$\frac{1}{2}(\omega_A + \omega_B) + \frac{1}{2}D + \frac{1}{2}J$
$-\frac{1}{2}D - \frac{1}{2}J$	$(1 - \sin 2\theta)\sin^2\left(\frac{\beta}{2}\right)\Sigma$			
$-\frac{1}{2}D$	$-\frac{1}{4}\cos^2 2\theta \sin^2\beta$	$-\frac{1}{4}\cos^2 2\theta \sin^2\beta$		
$-\frac{1}{2}D + \frac{1}{2}J$		$(1 + \sin 2\theta)\sin^2\left(\frac{\beta}{2}\right)\Delta$		
$-\frac{1}{2}J$	$-\cos^2 2\theta \sin^4\left(\frac{\beta}{2}\right)$		$-\cos^2 2\theta \sin^4\left(\frac{\beta}{2}\right)$	
0	$-\frac{1}{4}(1 - \sin 2\theta)^2 \sin^2\beta$	$-\frac{1}{4}(1 + \sin 2\theta)^2 \sin^2\beta$	$-\frac{1}{4}(1 + \sin 2\theta)^2 \sin^2\beta$	$-\frac{1}{4}(1 - \sin 2\theta)^2 \sin^2\beta$
$\frac{1}{2}J$		$-\cos^2 2\theta \sin^4\left(\frac{\beta}{2}\right)$		$\cos^2(2\theta)\sin^4\left(\frac{\beta}{2}\right)$
$\frac{1}{2}D - \frac{1}{2}J$			$(1 + \sin 2\theta)\sin^2\left(\frac{\beta}{2}\right)\Delta$	
$\frac{1}{2}D$			$-\frac{1}{4}\cos^2 2\theta \sin^2\beta$	$-\frac{1}{4}\cos^2 2\theta \sin^2\beta$
$\frac{1}{2}D + \frac{1}{2}J$				$(1 - \sin 2\theta)\sin^2\left(\frac{\beta}{2}\right)\Sigma$
$\frac{1}{2}(\omega_A + \omega_B) - \frac{1}{2}D - \frac{1}{2}J$	$(1 - \sin 2\theta)\cos^2\left(\frac{\beta}{2}\right)\Sigma$			
$\frac{1}{2}(\omega_A + \omega_B) - \frac{1}{2}D$	$\frac{1}{4}\cos^2 2\theta \sin^2\beta$	$\frac{1}{4}\cos^2 2\theta \sin^2\beta$		
$\frac{1}{2}(\omega_A + \omega_B) - \frac{1}{2}D + \frac{1}{2}J$		$(1 + \sin 2\theta)\cos^2\left(\frac{\beta}{2}\right)\Delta$		
$\frac{1}{2}(\omega_A + \omega_B) - \frac{1}{2}J$	$-\frac{1}{4}\cos^2 2\theta \sin^2\beta$		$-\frac{1}{4}\cos^2 2\theta \sin^2\beta$	
$\frac{1}{2}(\omega_A + \omega_B)$	$\frac{1}{4}(1 - \sin 2\theta)^2 \sin^2\beta$	$\frac{1}{4}(1 + \sin 2\theta)^2 \sin^2\beta$	$\frac{1}{4}(1 + \sin 2\theta)^2 \sin^2\beta$	$\frac{1}{4}(1 - \sin 2\theta)^2 \sin^2\beta$
$\frac{1}{2}(\omega_A + \omega_B) + \frac{1}{2}J$		$-\frac{1}{4}\cos^2 2\theta \sin^2\beta$		$-\frac{1}{4}\cos^2 2\theta \sin^2\beta$
$\frac{1}{2}(\omega_A + \omega_B) + \frac{1}{2}D - \frac{1}{2}J$			$(1 + \sin 2\theta)\cos^2\left(\frac{\beta}{2}\right)\Delta$	
$\frac{1}{2}(\omega_A + \omega_B) + \frac{1}{2}D$			$\frac{1}{4}\cos^2 2\theta \sin^2\beta$	$\frac{1}{4}\cos^2 2\theta \sin^2\beta$
$\frac{1}{2}(\omega_A + \omega_B) + \frac{1}{2}D + \frac{1}{2}J$				$(1 - \sin 2\theta)\cos^2\left(\frac{\beta}{2}\right)\Sigma$

Note. $\Sigma = \left[\cos^2\left(\frac{\beta}{2}\right) + \sin 2\theta \sin^2\left(\frac{\beta}{2}\right)\right]$; $\Delta = \left[\cos^2\left(\frac{\beta}{2}\right) - \sin 2\theta \sin^2\left(\frac{\beta}{2}\right)\right]$; $D = [J^2 + (\omega_A - \omega_B)^2]^{1/2}$; $\cos 2\theta = (\omega_A - \omega_B)/D$.

We would like to point out that for computational purposes it is also possible to relate SECSY spectra to 2D *J*-resolved spectroscopy. Signal intensities for a SECSY spectrum can then be computed from the expressions given by Kumar (*13*) for 2D *J*-resolved spectroscopy by setting the rotation angle of the second radio frequency pulse equal to 90°.

As a simple example of such a calculation, we present in Table 1 the frequencies and the intensities of a SECSY spectrum for a strongly coupled two-spin AB

system. A mixing pulse with rotation angle β is assumed. The table has been arranged to correspond pictorially to Fig. 5a′. The upper half contains the desired N-type peaks, while the lower half consists of the P-type peaks, which are suppressed by the extended scheme discussed in Section IV. The relative peak intensities of Table 1 can be obtained from the real amplitudes given by Eq. [61] of Ref. (*2*) taking into account that the complex amplitudes of Eq. [8] can be expressed by the real amplitudes of Ref. (*2*) as follows:

$$\begin{aligned}
\mathrm{Re}\{Z^{(x)}_{kl,mn}\} &= A_{(kl)(mn)} + B_{(kl)(mn)} \\
\mathrm{Re}\{Z^{(x)}_{kl,nm}\} &= A_{(kl)(mn)} - B_{(kl)(mn)} \\
\mathrm{Im}\{Z^{(x)}_{kl,mn}\} &= 0.
\end{aligned}$$

For the special case $\beta = 180°$, the peak intensities of Table 1 reduce to those collected in Table 4 of Ref. (*13*). For a weakly coupled spin system with $\theta = 0$ and $\beta = 90°$, all peaks have equal absolute intensities. It is important to note that the groups of four cross-peaks relating transitions of different nuclei have zero total intensity. For the weakly coupled two-spin case, this is true for all values of β, for the strongly coupled AB spin system only for $\beta = 90°$. This implies that the cross-peak intensities will mutually cancel when the multiplets are not resolved. Inherently broad lines or resolution limited by insufficient data points can lead to such a cancellation. None or extremely weak cross-peaks will occur for unresolved long-range couplings. This fact makes a SECSY spectrum of a biological macromolecule simple and interpretable. It can generally be observed that cross-peaks are often of rather low intensity due to partial cancellation of overlapping peaks.

Overlap of peaks due to field inhomogeneity does not lead to the above-mentioned cancellation. This arises from the virtue that the field inhomogeneity is partially refocused for N-type peaks in the ω_1 direction. On the other hand, P-type peaks do not experience such a refocusing effect and are generally broader than N-type peaks.

VI. CONCLUSIONS

It has been a surprise to the authors that despite the enormous number of cross-peaks to be expected in a 2D correlated spectrum of a large molecule, e.g., a protein, a quite informative presentation of the connectivity information can be obtained. It appears that 2D correlated spectroscopy in the particular forms described here will become a valuable tool for the elucidation of complex high-resolution NMR spectra.

ACKNOWLEDGMENTS

This research has been supported by a joint project of the Institut für Molekularbiologie and Biophysik and the Laboratorium für Physikalische Chemie granted by the Swiss Federal Institute of Technology. We would like to acknowledge receipt of a preprint by Dr. Luciano Müller describing foldover correction for 2D resolved carbon-13 spectroscopy.

REFERENCES

1. J. JEENER, Ampere International Summer School II, Basko Polje (1971).
2. W. P. AUE, E. BARTHOLDI, AND R. R. ERNST, *J. Chem. Phys.* **64,** 2229 (1976).
3. K. NAGAYAMA, K. WÜTHRICH, AND R. R. ERNST, *Biochem. Biophys. Res. Commun.* **90,** 305 (1979).
4. A. DE MARCO, H. TSCHESCHE, G. WAGNER, AND K. WÜTHRICH, *Biophys. Struct. Mech.* **3,** 303 (1977).
5. K. WÜTHRICH, G. WAGNER, R. RICHARZ, AND S. J. PERKINS, *Biochemistry* **17,** 2253 (1978).
6. R. BRACEWELL, "The Fourier Transformation and Its Applications," Chap. 6, McGraw–Hill, New York, 1965.
7. D. C. CHAMPENEY, "Fourier Transforms and Their Physical Applications," Academic Press, London/New York, 1973.
8. L. MÜLLER, *J. Magn. Reson.* **36,** 301 (1979).
9. W. P. AUE, J. KARHAN, AND R. R. ERNST, *J. Chem. Phys.* **64,** 4226 (1976).
10. K. NAGAYAMA, K. WÜTHRICH, P. BACHMANN, AND R. R. ERNST, *Biochem. Biophys. Res. Commun.* **78,** 99 (1977).
11. K. NAGAYAMA, P. BACHMANN, K. WÜTHRICH, AND R. R. ERNST, *J. Magn. Reson.* **31,** 135 (1978).
12. P. BACHMANN, W. P. AUE, L. MÜLLER, AND R. R. ERNST, *J. Magn. Reson.* **28,** 29 (1977).
13. ANIL KUMAR, *J. Magn. Reson.* **30,** 227 (1978); compare also the Erratum published in this number of *J. Magn. Reson.*